Neurobiology of Aging 136 (2024) 9–22

Contents lists available at ScienceDirect

Neurobiology of Aging

journal homepage: www.elsevier.com/locate/neuaging.org

Age-related similarities and differences in cognitive and neural processing revealed by task-related microstate analysis

Chandlyr M. Denaro [a], Catherine L. Reed [a,*], Jasmin Joshi [a], Astrid Petropoulos [b], Anjali Thapar [c], Alan A. Hartley [a]

[a] Claremont McKenna College, USA
[b] Carleton College, USA
[c] Bryn Mawr College, USA

ARTICLE INFO

Keywords:
Aging
Microstates
STAC-r
ERPs
N170
N400
ERN
P3

ABSTRACT

We explored neural processing differences associated with aging across four cognitive functions. In addition to ERP analysis, we included task-related microstate analyses, which identified stable states of neural activity across the scalp over time, to explore whole-head neural activation differences. Younger and older adults (YA, OA) completed face perception (N170), word-pair judgment (N400), visual oddball (P3), and flanker (ERN) tasks. Age-related effects differed across tasks. Despite age-related delayed latencies, N170 ERP and microstate analyses indicated no age-related differences in amplitudes or microstates. However, age-related condition differences were found for P3 and N00 amplitudes and scalp topographies: smaller condition differences were found for in OAs as well as broader centroparietal scalp distributions. Age group comparisons for the ERN revealed similar focal frontocentral activation loci, but differential activation patterns. Our findings of differential age effects across tasks are most consistent with the STAC-r framework which proposes that age-related effects differ depending on the resources available and the kinds of processing and cognitive load required of various tasks.

1. Introduction

Age-related differences in cognitive function have been associated with changes in performance (e.g., delayed responses to stimuli), brain function (e.g., decreased neural activation), and structure (e.g., reduced brain volume), among others (Grady, 2012). Physiological and brain imaging technologies have improved our understanding of these age-related differences (Reuter-Lorenz and Park, 2010). In particular, the use of electroencephalography (EEG) and event-related potentials (ERP) has allowed assessment of cognitive processes in real time by using sensors to measure voltage changes on the scalp (Banaschewski et al., 2007). However, few studies have examined whether age-related neural processing differences are consistent across cognitive tasks within individuals. Likewise, few studies have made use of new whole-head scalp topography analysis techniques to explore changes in the scalp distributions of neural processing associated with aging.

Examining ERPs of older and younger adults has identified age differences associated with a variety of cognitive processes (Yi and Friedman, 2011). The N170 elicited by faces, in contrast to objects, was delayed and larger in older relative to younger adults (Boutet et al., 2021). The P3 elicited to infrequent compared to frequent events increased in latency and decreased in amplitude with increasing age (van Dinteren et al., 2014). The N400 effect reflecting differences between semantically related and unrelated word pairs decreased with age (Joyal et al., 2020). The error related negativity (ERN) in a flanker task was reduced in older adults and had a somewhat different component structure (Hoffmann and Falkenstein, 2011). Generally, older adults are reported to produce smaller amplitudes and longer latencies than younger adults (Friedman, 2012). An important exception to the finding of smaller amplitudes in older adults comes from studies requiring inhibition of responses, such as Go/NoGo or stop signal procedures, in which greater activation has been found in older adults (Hong et al., 2014; Kropotov et al., 2016; Paitel et al., 2021; Staub et al., 2014).

ERP analysis has been an effective method of identifying age-related differences in the timing and strength of neural responses in various cognitive processes. However, conventional ERP analyses select sensors (or groups of sensors) and processing time windows based on a priori assumptions about the underlying neural generators of the ERPs,

* Correspondence to: Department of Psychological Science, Claremont McKenna College, 850 Columbia Ave Claremont, CA 91711, USA.
E-mail address: clreed@cmc.edu (C.L. Reed).

https://doi.org/10.1016/j.neurobiolaging.2024.01.007
Received 16 May 2023; Received in revised form 12 January 2024; Accepted 16 January 2024
Available online 20 January 2024

potentially limiting the hypotheses that can be addressed with ERPs, as well as missing age-related changes that may not be present at the electrode or time window of interest. Even when ERP analyses include a multi-electrode region of interest, they are limited in that they do not quantify synchronous activity across the whole head over time. Further, another limitation is that the presence of a particular component in the waveform and its amplitude are dependent on the reference that is chosen (Murray et al., 2008).

More recently, technological and computational advances have led to the development of analytic methods that identify distinct voltage distributions across scalp electrodes over time (Murray et al., 2008; Michel and Koenig, 2018). For example, microstate analysis of resting EEG data has identified periods ranging from tens to hundreds of milliseconds when the scalp topography remains stable (Tomescu et al., 2018). In contrast to ERP analyses, microstate analysis requires no a priori assumptions about the scalp location or timing of neural processes because it classifies stable configurations of voltage activity over time over the entire electrode array. Examination of these stable topographical patterns allows insights into the temporal dynamics of neural activity as well as insights into the organization of perceptual and cognitive processes in the brain. Different microstates are thought to reflect differing mental processes since each map displays activation from a different pattern of neural sources (Lehmann and Michel, 2011; Khanna et al., 2015; Koenig et al., 2005; Michel and Koenig, 2018). Thus, microstate analysis allows for the exploration of hypotheses regarding age-related differences in neural processing such as whether microstates differ by age or task conditions. More specifically, it can allow assessment of theories predicting topographic shifts toward more frontal activation (Davis et al., 2008) or reduced hemispheric asymmetry (Cabeza, 2002) for the cognitive processing of older adults.

Most microstate research has focused on resting-state EEG microstates in young adults in paradigms in which no specified cognitive operations are called for (Jabès et al., 2021; Zanesco et al., 2020.) In these studies, much of the variance in global field power (GFP)[1] can be explained by four to six microstates. In older adults, the same microstates are observed although they occur less frequently, with longer durations (Jabès et al., 2021; Koenig et al., 2002; Tomescu et al., 2018). Specifically, Jabes et al., Koenig et al., and Zanesco et al. reported a lower occurrence of one of the major states (State C) in older adults, although Tomescu et al. did not find this. State C shows strong occipital and parietal activation and has been linked to neuronal activity in parietal brain regions, in particular core regions of the default mode network (Custo et al., 2017). Jabès et al. and Zanesco et al. also found lower activity in another state (referred to as C' by Jabes et al., 2021 or E by Zanesco et al., 2020) linked to the cortical salience network. This state extends more centrally than State C.

Importantly, microstate analysis can also be used to explore task-related cognition (Koenig et al., 2011). Most of these studies use task-related data from young adults (Jouen et al., 2021; Kim et al., 2021). We are aware of only one study using task-related microstate analysis to compare younger and older adults, in this case using the Stroop procedure (Ménétré and Laganaro, 2023). When comparing microstate maps for younger and older adults, the same microstate maps were present for both age groups. Although older adults showed a general slowing of the onset of the states, age-related differences emerged in the duration of the conflict detection phase around 400 ms, such that older adults had a disproportionately longer state duration. Based on a source reconstruction, Ménétré and Laganaro concluded that a relatively similar network of structures was engaged in both age groups.

In this study, we examined age-related differences across four different cognitive tasks, some more perceptual and others more cognitive, performed by the same participants. We used well-studied paradigms that produce ERPs with well-documented timing, neural distributions, and neural sources: (1) a visual discrimination task for eliciting the face-specific N170 response (Eimer, 2011; Feuerriegel et al., 2015; Rossion and Jacques, 2012); (2) an active visual oddball paradigm for eliciting the P3 component (van Dinteren et al., 2014; Polich, 2007, 2012); (3) a word-pair association paradigm for eliciting the N400 component (Kutas and Federmeier, 2011; Lau et al., 2008; Swaab et al., 2011); and (4) a flanker paradigm for eliciting the error related negativity, or ERN (Gehring et al., 2012; Olvet and Hajcak, 2008). We expected to replicate age-related ERP differences reported in the literature and determine whether these differences could be confirmed when the same participants performed all four tasks.

The central goal and the novel contribution of the present research was to explore the microstate concomitants of these ERPs. We compared the ERP results with those from task-related microstate analyses to determine if age-related differences in scalp topographies converged with ERP findings and whether the whole-scalp configuration of these microstates could tell us more about age-related changes in neural processing.

2. Method

2.1. Participants

Forty participants were recruited from the Claremont Colleges and the surrounding Claremont, CA (USA) community. Younger adults (YA) received either financial compensation or partial course credit; older adults (OA) received financial compensation. Compensated participants were paid $10 per hour. All participants had at least 20:30 vision, measured using a vision contrast test (Vistech Consultants, Inc.). No participant reported a history of psychological disorders, neurological injury or disease, loss of consciousness for more than two minutes, or stroke. The study was approved by the Claremont McKenna College Institutional Review Board. All participants provided informed consent. The Shipley Institute of Living Scale (SILS) assessed general levels of intellectual functioning with vocabulary and abstraction subscales (Shipley and Burlingame, 1941). YAs and OAs did not differ in the combined score, t (32) = 1.47, p = 0.15. No participants scored below the cut-off score of 21 in the vocabulary assessment, indicating participants did not have impaired cognitive function (Harnish et al. (1994). However, it is of note that OAs had higher Vocabulary scores than YAs, t (32) = −2.80, p = 0.01, but YAs had higher Abstraction scores than OAs, t (32) = 3.50, p = 0.001.

Participants were excluded from analyses based on data quality and task performance across all four tasks. Poor data quality was determined if at least one data set had less than 50% of trials remaining after artifact rejection and correction, or significant noise remained in the data following artifact correction (n = 3 YA). Poor performance was determined if task accuracy was under 70% in any task (n = 3 OA). For the flanker task, all participants met the inclusion criterion of at least six errors (Kappenman et al., 2021). Thus, 34 participants were included in analyses with 17 YAs and 17 OAs. The demographics of the participants are listed in Table 1.

2.2. Tasks

2.2.1. Procedure

Participants completed four experimental tasks while EEG was collected: Face Perception, Active Visual Oddball, Word-Pair Judgment, and Flanker tasks (modified from Kappenman et al., 2021; Fig. 1).

[1] Global field power (GFP) is a reference-independent measure of the potential field. It quantifies the amount of activity at each time point in the field, integrating the data from all recording electrodes simultaneously (Skrandies, 1990). It corresponds to the spatial standard deviation in an electrical potential map at a given point in time. Low GFP is associated with relatively uniform activity; high GFP is associated with substantial variability in activity across the scalp.

Table 1
Participant demographic data (n = 34).

Group	N (# of females)	Mean age in years (*SD*) range	Mean years education (*SD*)	SILS* : mean score (*SD*)	SILS: mean vocabulary (*SD*)	SILS: mean abstraction (*SD*)
Young Adults	17 (7)	20.76 (1.25) 19-23	15.06 (1.03)	69.44 (5.36)	32.85 (3.59)	36.59 (2.62)
Older Adults	17 (8)	72.19 (3.77) 66-79	19.75 (2.49)	65.46 (9.80)	35.93 (2.77)	29.53 (7.89)

*SILS= Shipley Institute of Living Scale.

Participants were seated at a viewing distance of 75 cm from the screen, with eyes level with the center of the screen, legs uncrossed, and feet flat on the floor. Stimuli were presented on a ViewPixx computer monitor with a 61.5 cm screen with a 1280×1024 resolution (Vision Science Solutions) using Presentation version 22 software (Neurobehavioral Systems). Task order was counterbalanced across participants. The EEG testing session was approximately 1.5 h in duration.

2.2.2. Face Perception

The face perception task was an object recognition paradigm modified from Rossion and Caharel (2011) (Fig. 1a). Face images were modified to remove background, clothing, and hair. Car images were edited to remove the background. Scrambled faces and scrambled cars were created using a Fourier phase randomization procedure (Jacques and Rossion, 2004). On each trial, a stimulus was presented from one of four categories: faces, cars, scrambled faces, and scrambled cars. Each stimulus subtended 3.32° × 3.78° of visual angle and was presented in the center of the screen for 300 ms, with a jittered ISI of 1100–1300 ms (rectangular distribution, average of 1200 ms). A central white fixation point (0.15° visual angle) was presented during the ISI. Faces and cars were referred to as "objects," and scrambled faces and scrambled cars were referred to as "textures." Participants pressed one button for objects and another button for textures using the index and middle fingers of their dominant hand. The stimulus-response mapping was counterbalanced across participants, such that half of the participants pressed with the index finger for objects, and half of the participants pressed with the index finger for textures. Each stimulus category had 40 stimuli, presented twice, for a total of 320 trials. Stimuli were presented in a random order, with the exception that a given stimulus was only presented once in the first half and once in the second half of the experiment. Participants were given a rest break every 40 trials.

2.2.3. Visual oddball

For the active visual oddball task, participants viewed a sequence of letter stimuli and classified each stimulus as a target or non-target. On each trial, a letter (A, B, C, D, E, in uppercase, Geneva font, subtending 2.5×2.5° of visual angle) was presented for 200 ms in the center of the screen over a continuously visible central white fixation point (0.15° visual angle), with a jittered SOA of 1200 - 1400 ms (rectangular distribution, average of 1300 ms). Participants pressed one button for targets and another button for non-targets using the index and middle fingers of their dominant hand (Fig. 1b). Prior to each block of trials, one letter was designated as the target stimulus and the other four letters were non-targets. Each of the five letters served as a target in one block of the experiment and as a non-target in the other four blocks, with the order of blocks randomized across participants. The stimulus-response mapping was counterbalanced across participants (50% of participants used the index finger for targets; 50% of participants used the index finger for non-targets). Participants completed five blocks with 40 trials each, for a total of 200 trials. In each block, the probability of the target was 20%, and the probability of the non-targets was 80%, for a total of 8 target trials and 32 non-target trials per block. The probability of each of the non-targets and targets within a block was 20%, eliminating possible sensory differences between target and non-target stimuli. Breaks were provided between blocks to allow participants to rest their eyes.

2.2.4. Word-pair judgment

For the word-pair judgment task, participants determined if two words were semantically related (see Kappenman et al., 2021 Supplement for list of words). The two words were presented in different colors of ink to make it easier for participants to track which word required a response. Both colors were equally distant from the gray background in the CIE (1976) color space. Words were presented in uppercase, Geneva font, with each letter in a word subtending 1×1° of visual angle. Each word was presented over a continuously visible white central fixation point (0.15° visual angle).

The first word on each trial ("prime") was presented in red (100, 0, 0) for 200 ms, followed by an ISI of 900–1100 ms (rectangular distribution, average of 1000 ms). The second word ("target") was then presented in green (0, 90, 0) for 200 ms, followed by an ITI of 1400 - 1600 ms (rectangular distribution, average of 1500 ms) (Fig. 1c). Participants pressed one button for related word pairs and another button for unrelated word pairs using the index and middle fingers of the dominant hand. The stimulus response mapping was counterbalanced across participants (50% of participants pressed with the index finger for related word pairs; 50% of participants pressed with the index finger for unrelated word pairs. Each target word was presented once in a related word pair and once in an unrelated word pair. Word pairs were randomly intermixed. Participants completed 120 trials, with a break provided every 20 trials.

2.2.5. Flanker

The flanker task was modified from the Eriksen flanker task (Eriksen and Eriksen, 1974). In each trial, a central arrowhead was flanked by two arrowhead stimuli on either side all in black for 200 ms over a continuously visible central white fixation point (0.15° visual angle), with a jittered SOA of 1200 - 1400 ms (rectangular distribution, average of 1300 ms). Each arrowhead stimulus subtended 1° of visual angle. Participants made either a left-hand or right-hand button press corresponding to the direction of the central arrowhead (Fig. 1d). Flanker stimuli either pointed in the same direction (congruent trials) or the opposite direction (incongruent trials) as the target stimulus. Participants completed a total of 400 trials, with a break provided every 40 trials. Leftward and rightward pointing targets each occurred on half of the trials, and congruent and incongruent flankers each occurred on half of the trials; all trial types were randomly intermixed. To ensure an adequate number of error trials, feedback saying "Try to respond a bit faster" if the error rate dipped below 10%, or "Try to respond more accurately" if the error rate exceeded 20% was presented during the break between trial blocks. If the error rate was between 10–20%, a message of "Good job!" was presented. Because the leftward and rightward pointing arrowhead stimuli are strongly associated with left- and right-hand responses, respectively, the stimulus-response mapping was held consistent across participants.

2.3. Electrophysiological methods

Continuous scalp electroencephalograms (EEGs) were recorded from 32 active Ag/AgCl electrodes (actiCAP, Brain Products GmbH, Gilching, Germany) using the Brain Vision actiCHamp system (actiCHamp, Brain Products GmbH, Gilching, Germany). Impedances were kept below

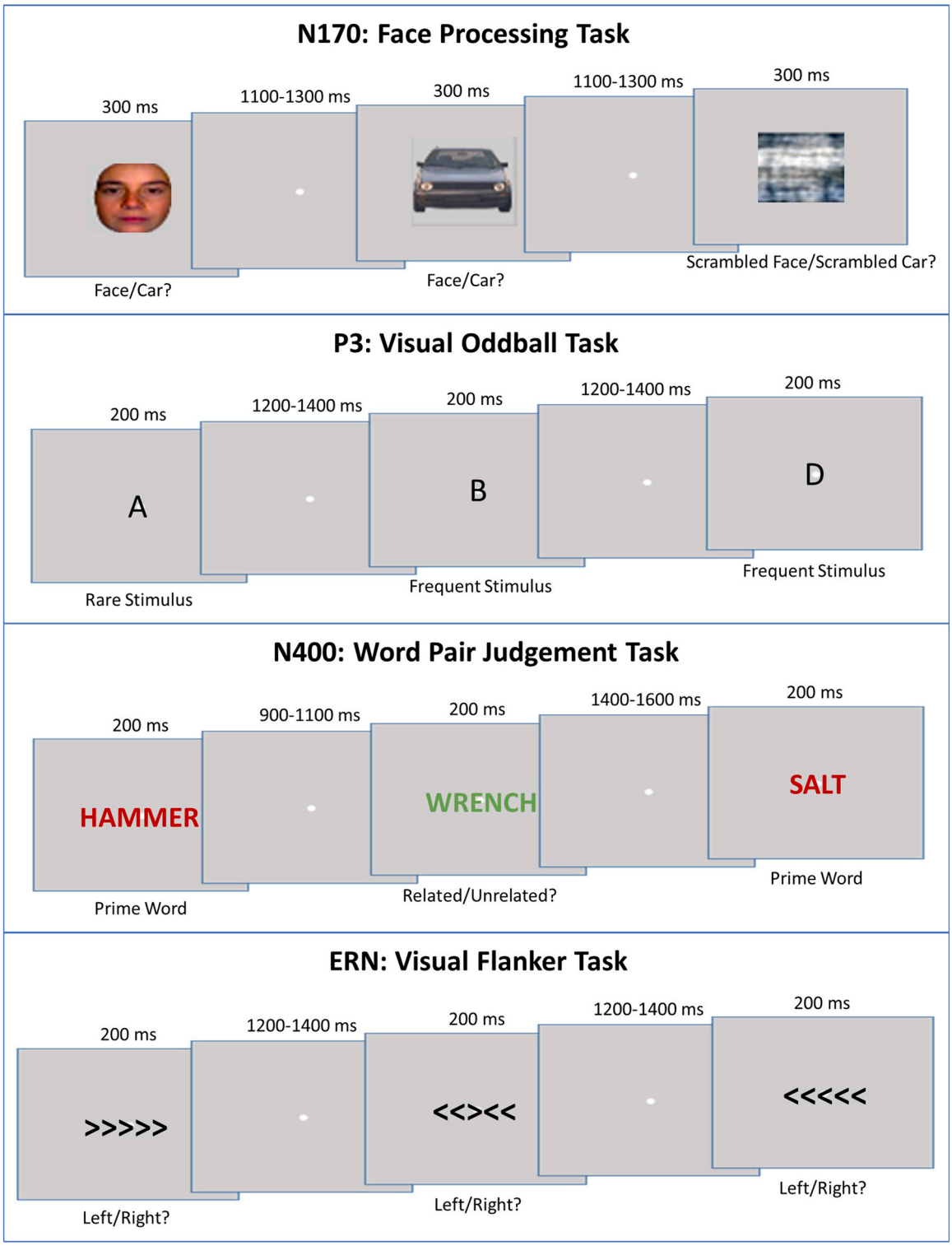

Fig. 1. Four tasks: face perception, visual oddball, word pair judgment, and visual flanker. (modified from Kappenman et al., 2021).

50 kΩ throughout the experiment. Electrodes were placed at Fp1, Fp2, F3, Fz, F4, F7, F8, FC3, FC4, C3, Cz, C4, C5, C6, TP9, CPz, TP10, P3, Pz, P4, P7, P8, P03, P04, P07, P08, 01, Oz, O2 according to the international 10/10 system. The horizontal electrooculogram (HEOG) was recorded from electrodes placed lateral to the external canthi and the vertical electrooculogram (VEOG) was recorded from an electrode placed below the right eye. The continuous EEG was digitized at 500 Hz.

2.3.1. EEG data analysis and reduction

Data were imported into MATLAB and analyzed using the EEGLAB toolbox (Delorme et al., 2004) and ERPLAB toolbox (http://www.erpinfo.org/erplab). EEG data were adjusted for DC bias then filtered using an IIR Butterworth band-pass filter from 0.1 to 30 Hz (12 dB/oct half amplitude cut off, 40 dB/dec roll-off). Data were re-referenced off-line to the average of TP9 and TP10 mastoid electrodes for the Visual Oddball, Word Pair Judgment, and Flanker tasks, and to an average

reference for the Face Perception task (Wang et al., 2019). None of the data sets contained bad channels. Continuous data were segmented into epochs. For the face perception, visual oddball, and word pair judgment tasks, segments were stimulus locked and defined from 200 ms pre-stimulus to 600 ms post-stimulus. For the flanker task, data were response locked and defined for 400 ms post response with a baseline from − 600 to − 400 ms before the response. For all tasks, baseline correction used the mean voltage from a 200 ms pre-stimulus or pre-response period. Artifacts in the data were addressed in two ways. First, trials were removed from analysis if they contained significant ocular artifacts (+/- 100 μV at HEOG or VEOG) during stimulus presentation (+/- 150 ms surrounding stimulus presentation). Second, ocular (eye blink, eye movement), muscle and electrical artifacts were identified and corrected for the entire trial length (200 ms pre-stimulus to 600 ms post-stimulus) using independent component analysis (ICA, method RUNICA; Jung et al., 2000; Delorme et al., 2007). ICLabel (Pion-Tonachini et al., 2019) and SASICA (Chaumon et al., 2015) were used for independent confirmation of artifact components to be removed. For each participant's cleaned EEG data set, the trials were averaged for each task condition for ERP analyses.

2.3.2. Behavioral and ERP data analysis

For each experimental task, we analyzed behavioral measures (proportion accuracy, mean correct response time, and/or number of errors). For the stimulus-locked N170, P3, and N400 components, we analyzed ERP mean amplitudes for correct trials only; the time windows for the mean amplitude quantification were based on examination of the grand average data averaged across conditions as well as the time windows reported in the literature (Kappenman et al., 2021). For the flanker task, we measured pre- (−110 to 0 ms) and post-response (−0 to 110 ms) mean amplitudes for correct and error (ERN) responses from participants' average ERP waveforms. We calculated the difference between pre- and post-response mean amplitudes by subtracting the post-response mean amplitude from the pre-response mean amplitude.

For each experiment we confirmed that the majority of the data were represented within the selected time windows. For each task, we conducted mixed-model analyses of variance (ANOVAs) with the between-subjects factor of Age (YA, OA) and the within-subjects factor of Condition (2). The N170 analysis also included an Electrode (2) factor to examine age-related differences in the lateralization of face processing (Rossion et al., 2003). Effect sizes are partial eta squared (η_p^2).

2.3.3. Topographic data analysis

For microstate analysis, we employed the Randomization Graphical User Interface (RAGU; http://www.thomaskoenig.ch/index.php/work/ragu/1-ragu; see Koenig et al., 2011 for a complete description of the methods; Murray et al., 2008 for a tutorial) to conduct multivariate statistical analyses of multichannel event-related data. These analyses are based on measures of scalp field differences and include all sensors in the randomization statistics to extract stable and recurring topographic patterns of electrical activity on the scalp. They make no a priori assumptions regarding the latency or location of maximal neural activity. Baseline-corrected, time x channel data were normalized to eliminate differential spatial distributions between the maps. Analysis of each task comprised a between-subjects Age (YA, OA) factor and a within-subjects Condition (2) factor.

Three types of topographic ERP analyses were conducted. First, a topographic consistency test (TCT) evaluated whether there was consistent neural activity in the conditions across all participants most of the time by testing the null hypothesis that consistency between subjects is relatively small and produced by chance. For both age groups in all conditions across all four tasks, the TCT confirmed that over 80% of the data had consistent neural activation ($p < 0.0002$), indicating that consistency between participants' datasets was not produced by chance.

Next, a topographic analysis of variance (TANOVA), a nonparametric analysis of the global dissimilarities between topographical maps, was conducted to test whether the different experimental conditions elicited different brain functional states at given time points. Specifically, the dissimilarity in topographic maps is calculated for each point in time. In our study we calculated dissimilarity maps for age groups, conditions, and the interaction between age group and condition (i.e., the condition differences within each age group). Randomization tests were carried out to determine whether there were significant differences in the microstate patterns that could not be produced by chance. For example, for the main effect of condition, data points are randomly reassigned to conditions and the differences between these artificial groups were calculated. In our study, this procedure was repeated 5000 times, creating a distribution of the differences to be expected under the hypothesis of no condition effect. The likelihood that the actual differences that were observed occur in this distribution was determined. If the probability was less than or equal to 0.05, we concluded that the topographies of the conditions were significantly different at that point in time. This process was repeated for every point in time and extended periods with significant dissimilarities were identified. Thus, a significant TANOVA could indicate one of several possibilities. The two groups or conditions may have consistently different states (e.g., AAAA vs BBBB). They may have a variety of states that differ (e.g., ABCD vs EFGH). Or, they may have the same states but shifted in time. The time periods for significant Age by Condition interactions are reported in the Results section for each task.

Third, if TCT shows consistent neural activity, then it is appropriate to carry out microstate analysis. Microstate analysis is an examination of brain electromagnetic scalp data in terms of a set of fixed maps, quantifying the data by the time periods when each map is predominant (Brandeis et al., 1995). Specifically, microstate analysis looks for high spatial correlations between the topographic distribution of activity at two data points. (A data point is the activity of all electrodes at a point in time.) Data points with high correlations are clustered together. The clustering is iterative, with each new data point assigned to the cluster with which it has the highest correlation. For each pattern of clusters, the Global Explained Variance (GEV) is calculated. The number of clusters is reduced by identifying the cluster whose removal least penalizes the GEV. The number of clusters to retain is selected by the researcher based on the "elbow" at which the rate of improvement by adding another cluster drops. These patterns of electrode clusters yield a set of scalp maps that represent the different microstates. Each group and factor level at each moment in time is assigned to the microstate with which it has the highest spatial correlation. Statistics can be obtained for the onset and offset latency as well as the duration of each microstate. In addition, the mean GFP and the area under the GFP curve can be used to characterize the microstate. We also calculated center of gravity (COG), the GFP weighted by time. Duration, Area under the curve (AUC) and mean GFP of the microstates are considered global measurements of the occurrence of particular microstates. Onset, offset and center of gravity provide information about the behavior of the specific microstate in time; center of Gravity (COG) is a more robust temporal measure (Murray et al., 2008).

The RAGU output from microstate analysis (e.g., Fig. 3) shows scalp maps corresponding to each microstate (identified by a state number and a color) as well as the unfolding of the microstates (and the GFP) over the course of the epoch. To more closely examine the microstate sequence in a period of interest, we carried out a second microstate analysis focused on the combined YA and OA time window for the ERP for that experiment. In sum, microstate analysis can investigate whether certain brain processes, as indicated by the microstate maps, differ in their timing between factor levels (i.e., if their length, onset, or offset latency was affected by the experimental condition or group).

3. Results

For each task, behavioral analyses for proportion accuracy and correct response times (RTs; Table 2), ERP amplitude analyses (Table 3),

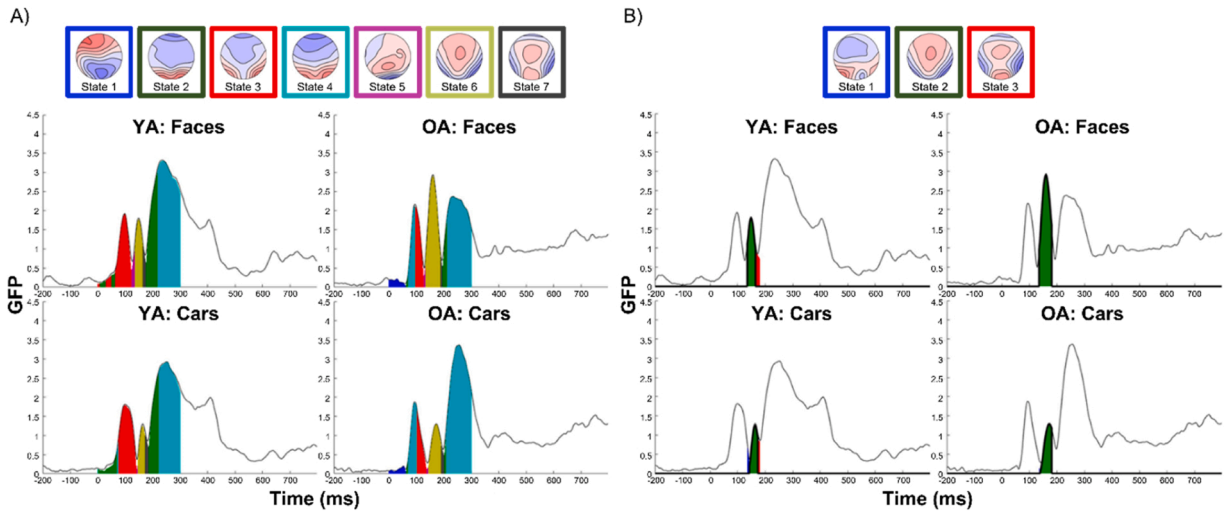

Fig. 3. Face Perception microstate output for younger (YA; left) and older (OA; right) adult groups by Face (upper) and Car (lower) conditions. A) Seven states explain 93.10% of total variance for the 0–300 ms time period. B) Three states explain 90.70% of total variance between 135–180 ms.

Table 2
Proportion accuracy and correct response time (RT) ANOVA results for N170, P3, and N400 experiments (df1 =1, df2 =32).

Experiment	Measure	Effect	F-value	P-value	η_p^2
N170	Accuracy	Age	8.24	0.01	0.21
		Condition	24.79	< 0.001	0.44
		Age x Condition	6.12	0.02	0.16
	RT	Age	16.80	< 0.001	0.34
		Condition	44.56	< 0.001	0.58
		Age x Condition	0.26	0.62	0.01
P3	Accuracy	Age	0.001	0.97	< 0.001
		Condition	47.67	< 0.001	0.60
		Age x Condition	0.79	0.38	0.02
	RT	Age	48.00	< 0.001	0.60
		Condition	35.59	< 0.001	0.53
		Age x Condition	0.40	0.53	0.01
N400	Accuracy	Age	0.30	0.59	0.01
		Condition	0.30	0.59	0.01
		Age x Condition	0.02	0.89	< 0.001
	RT	Age	10.90	0.002	0.25
		Condition	154.73	< 0.001	0.83
		Age x Condition	2.18	0.15	0.06

df = degrees of freedom. η_p^2 = partial eta squared

Table 3
Amplitude ANOVA results for N170, P3, N400 and ERN experiments (df1 =1, df2 =32).

Experiment	Effect	F-value	P-value	η_p^2
N170†	Age	2.12	0.16	0.06
	Condition	28.84	< 0.001	0.47
	Hemisphere	9.68	0.004	0.23
	Age x Condition	3.48	0.07	0.10
	Age x Hemisphere	1.34	0.26	0.04
	Condition x Hemisphere	1.24	0.27	0.04
	Age x Condition x Hemisphere	1.39	0.25	0.04
P3†	Age	6.31	0.02	0.17
	Condition	90.90	< 0.001	0.74
	Age x Condition	5.29	0.03	0.14
N400†	Age	2.72	0.11	0.08
	Condition	74.53	< 0.001	0.70
	Age x Condition	5.69	0.02	0.15
ERN††	Age	1.79	0.19	0.05
	Condition	9.22	0.005	0.23
	Age x Condition	4.89	0.03	0.13

df = degrees of freedom. η_p^2 = partial eta squared
† = mean amplitudes †† = peak-to-peak mean amplitudes

and topographic ERP analyses are reported. For all effects, means and standard errors (in parentheses) are reported.

3.1. Face perception (N170)

3.1.1. Behavior

Age x Condition ANOVAs were conducted for proportion correct and correct RT. The Age by Condition interaction showed that OAs had similar high accuracy for faces and cars, but YAs performed relatively better for faces, $M_{OA\text{-}faces}$ = 0.98 (0.01); $M_{OA\text{-}Cars}$ = 0.96 (0.01), $M_{YA\text{-}Faces}$ = 0.97 (0.01), $M_{YA\text{-}cars}$ = 0.90 (0.02). Overall, OAs performed the task more slowly than YAs, M_{OA} = 477 ms (16), M_{YA} = 391 ms (14), and faces were faster than cars, M_{Faces} = 422 ms (*15*), M_{Cars} = 446 ms (*15*). There was no Age by Condition interaction.

3.1.2. N170 amplitude analyses

N170 time windows were identified separately for YAs (135 - 175 ms) and OAs (140 - 180 ms) (Rossion and Caharel, 2011) and then mean amplitudes were extracted for correct responses to faces and cars at PO7/Left Hemisphere (LH) and PO8/Right Hemisphere (RH) (Fig. 2).

Overall, amplitudes were more negative for older adults than younger adults, M_{OA} = *−2.98* μV *(0.66)*, M_{YA} = *−0.69* μV *(0.93)*. The Age by Condition (Faces, Cars) by Hemisphere (PO7/LH, PO8/RH) ANOVA (Table 3) confirmed an N170 effect: faces elicited greater negative amplitudes than cars, M_{Faces} = −3.24 μV (0.54), M_{Cars} = −1.38 μV (0.51). In addition to greater negativities in RH than LH, the Condition by Hemisphere interaction showed a greater RH N170 for faces than cars, $M_{Faces\text{-}RH}$ = −3.85 μV (0.56), $M_{Faces\text{-}LH}$ = −2.63 μV (0.53), $M_{Cars\text{-}RH}$ = −1.78 μV (0.55), $M_{Cars\text{-}LH}$ = −0.99 (0.47). Although OAs had more negative N170s than YAs, M_{OA} = −2.97 μV (0.65); M_{YA} = −1.65 μV (0.80), age did not interact with condition, hemisphere or produce a three-way interaction.

3.1.3. Topographic microstate analyses

The TANOVA revealed a significant Age by Condition interaction between 144 to 188 ms explaining 15.15% of the variance ($p < 0.05$). The microstate analysis produced seven distinct states for Face and Car conditions between 0 to 300 ms that were shared by both age groups and explained 93.10% of the total variance in GFP (Fig. 3a). The timing and topography of State 6 resembled the bilateral occipitotemporal distribution of the N170 (Rossion and Jacques, 2008). Constraining microstate analysis to the 135 to 180 ms time period to include the ERP time periods for both age groups, a three-microstate model explained 90.70%

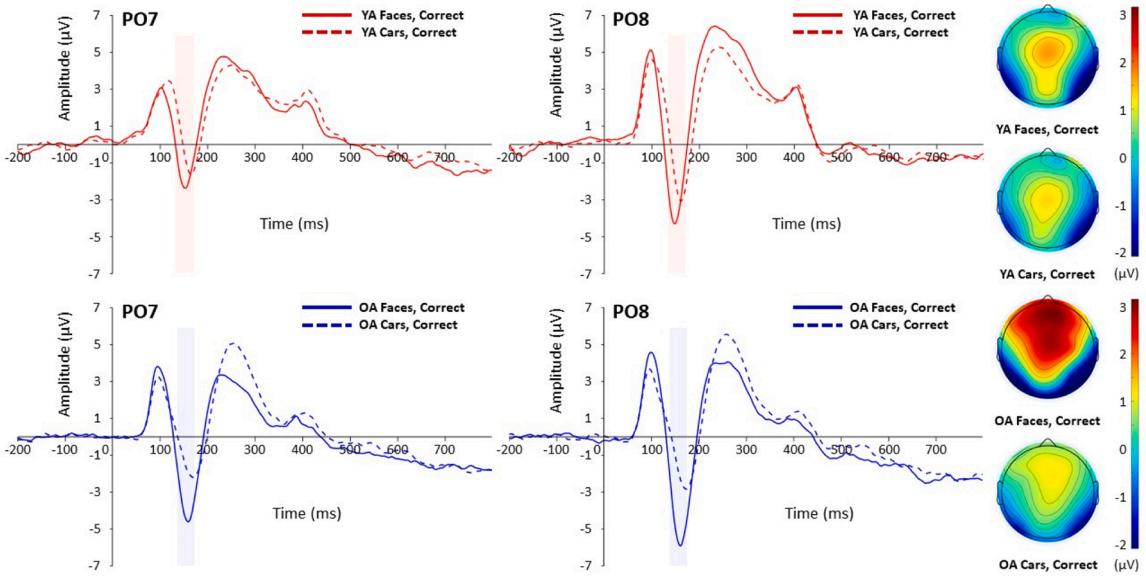

Fig. 2. Face perception/N170: Grand average waveform plots for Face and Car conditions produced by younger (YA) and older (OA) adults at PO7/LH and PO8/RH. Shaded areas indicate the N170 time window. Scalp maps represent average voltage for the ERP time window.

of the GFP variance (Fig. 3b). State 2 was similar to State 6 in the full analysis. There were no significant age-related State 2 onset differences, but there was a significant State 2 offset difference ($p < 0.02$) with State 2 for OAs ending later than for YAs. There were also corresponding increases in the OA's State 2 in terms of overall duration ($p = 0.03$) and COG ($p = 0.05$). State 2's AUC was greater for faces than cars ($p < 0.003$).

3.2. Visual oddball (P3)

3.2.1. Behavior

Age x Condition ANOVAs were conducted for proportion correct and correct RT. YAs and OAs performed with similar accuracy, $M_{OA} = 0.94$ (0.01), $M_{YA} = 0.94$ (0.01), and participants were more accurate for Frequent than Rare conditions, $M_{Frequent} = 0.98$ (0.01), $M_{Rare} = 0.90$ (0.02), but there was no interaction. OAs performed the task more slowly than YAs, $M_{OA} = 490$ ms (15), $M_{YA} = 369$ ms (11), and Rare

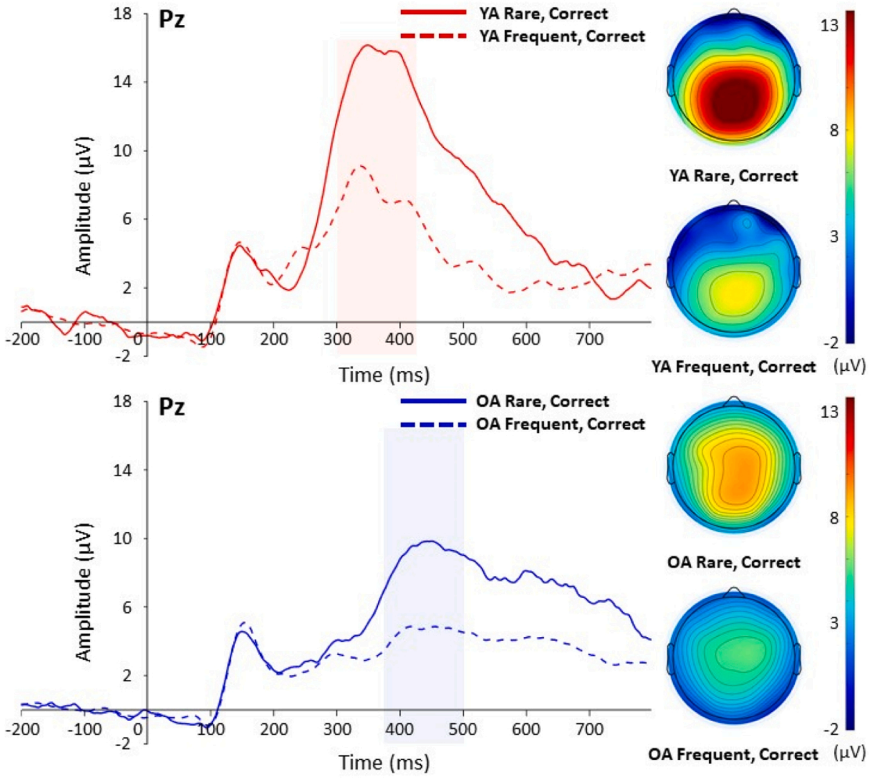

Fig. 4. Visual oddball/P3: Grand average waveform plots for correct Rare (target) and Frequent (non-target) conditions produced by younger (YA) and older (OA) adults at Pz. Shaded areas indicate the P3 component time window. Scalp maps represent average voltage for the ERP time window.

conditions were slower than Frequent conditions, M_{Rare} = 451 ms (15), $M_{Frequent}$= 408 ms (12), but there was no interaction.

3.2.2. P3 amplitude analyses

P3 time windows were identified separately for YA (300 - 425 ms) and OA groups (375 - 500 ms) (Polich, 2012) and mean amplitudes were calculated for Rare and Frequent conditions at Pz. The Age by Condition (Rare, Frequent) ANOVA (Fig. 4) showed lower amplitudes overall for OAs than YAs, M_{OA}= 6.85 μV (0.77), M_{YA}= 11.37 μV (1.64). The Condition difference confirmed the P3 effect, M_{Rare} = 12.10 μV (1.41), $M_{Frequent}$ = 6.13 μV (1.00). The significant Age by Condition interaction showed P3 effects were greater for YAs than OAs, $M_{YA\text{-}Rare}$ = 15.08 μV (1.85), $M_{YA\text{-}Frequent}$ = 7.67 μV (1.43), $M_{OA\text{-}Rare}$ = 9.12 μV (0.98), $M_{OA\text{-}Frequent}$ = 4.59 μV (0.57), but the interaction indicated that the age-related difference was greater for Rare than for Frequent conditions: YA_{Rare} vs OA_{Rare}: $t(32) = 2.71$, $p = 0.05$; other post-hoc comparisons, *ns*.

3.2.3. Topographic microstate analyses

The TANOVA revealed a significant Age by Condition interaction between 244 to 314 ms, explaining 13.18% of variance ($p < 0.03$). The fitting of microstate maps between 0 to 700 ms resulted in 9 distinct states explaining 93.95% of the total variance in GFP. Microstate maps between 300 to 500 ms produced 3 states explaining 95.65% of total variance in GFP. There were clear age-related timing and topographical differences across microstates. State 2 corresponded to State 4 in the full epoch, indicating a tight centroparietal topographical distribution associated with the P3 ERP voltage scalp distribution. This was the predominant state for YAs, but it was also present in OAs although diminished. There were significant condition effects of State 2 onset ($p = 0.001$) with the Frequent condition starting before the Rare condition. The significant offset effect for age group and condition effects indicated that State 2 had a much longer duration for YAs than OAs, as well for Frequent conditions. The mean GFP ($p = 0.01$) and AUC ($p = 0.005$) indicated Age by Condition interactions: State 2 was stronger for Frequent compared to Rare conditions in YAs, but was weaker and similar across conditions for OAs. In contrast, State 3, representing a more anterior centroparietal positivity, was the predominant state for OAs, although it was also present in YAs. It corresponded with State 5 in the longer epoch. State 3 had significant timing effects that did not interact with Age Group. The significant onset and duration effects for Age Group ($p < 0.006$) indicated that State 3 occurred earlier for YAs and lasted longer for OAs. The significant COG effect for group indicated it was later and longer for OAs. Condition effects showed timing differences for State 3 in the onset ($p = 0.02$) indicating it occurred earlier for Frequent conditions; the duration effect ($p = 0.03$) indicated it lasted longer for the Rare condition. Overall, the Frequent condition had a stronger mean GFP than the Rare condition ($p < 0.0001$). Thus, microstate analysis showed that age influenced the timing of the brain processes associated with attention and categorization as indicated by states for the different conditions. Nonetheless, age groups primarily differed in the predominant topographical state: the tight centroparietal topography that was predominant for YAs differed from the broader, slightly more anterior centroparietal topography predominant for OAs (Fig. 5).

3.3. Word-pair judgment (N400)

3.3.1. Behavior

Age x Condition ANOVAs were conducted for proportion correct and correct RT data. OAs performed with similar accuracy as YAs, M_{OA} = 0.98 (0.01); M_{YA} = 0.97 (0.01), and participants had similar accuracy for Related and Unrelated conditions, $M_{Related}$ = 0.97 (0.01), $M_{Unrelated}$ = 0.98 (0.01). There was no interaction. OAs performed the task more slowly than YAs, M_{OA} = 738 ms (30), M_{YA} = 594 ms (34), and Related word pairs had faster RTs than Unrelated word pairs, $M_{Related}$ = 589 ms (30), $M_{Unrelated}$ = 743 ms (34), but there was no interaction.

3.3.2. N400 amplitude analyses

Separate N400 time windows were identified for YA (260 - 460 ms; Kutas and Hillyard, 1980) and OA groups (350 - 550 ms) and mean amplitudes were calculated for each condition at Pz (Fig. 6). An Age by Condition (related, unrelated) ANOVA showed that amplitudes did not differ by age, M_{OA} = 2.46 μV (0.62), M_{YA} = 5.48 μV (1.40). The N400 effect was confirmed, with Unrelated amplitudes relatively more negative than Related amplitudes, $M_{Unrelated}$ = 1.50 μV (0.63), $M_{Related}$ = 6.89 μV (0.94). The significant Age by Condition interaction occurred because the N400 effect (i.e., Unrelated- Related difference) was larger for YAs than for OAs, $M_{YA\text{-}Related}$ = 9.03 μV (1.68), $M_{YA\text{-}Unrelated}$ = 1.93 μV (1.12), $M_{OA\text{-}Related}$ = 4.47 μV (0.70), $M_{OA\text{-}Unrelated}$ = 0.45 μV (0.54).

3.3.3. Topographical microstate analyses

The TANOVA analysis revealed a significant Age by Condition interaction between 390 to 536 ms which explained 14.89% of variance ($p < 0.03$). The fitting of microstate maps between 0 to 800 ms resulted in eight distinct states that explained 90.75% of the total variance in GFP

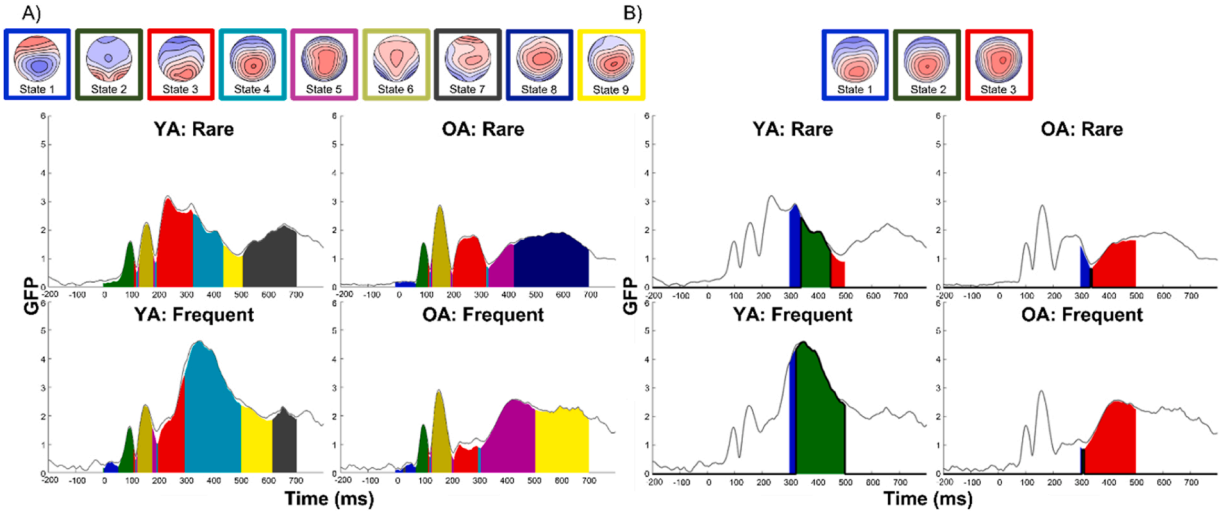

Fig. 5. Visual Oddball microstate output for younger (YA; left) and older (OA; right) adult groups by Rare (upper) and Frequent (lower) conditions. A) Nine states explain 93.95% of total variance for the 0–800 ms time period. B) Three states explain 95.65% of total variance between 300 - 500 ms.

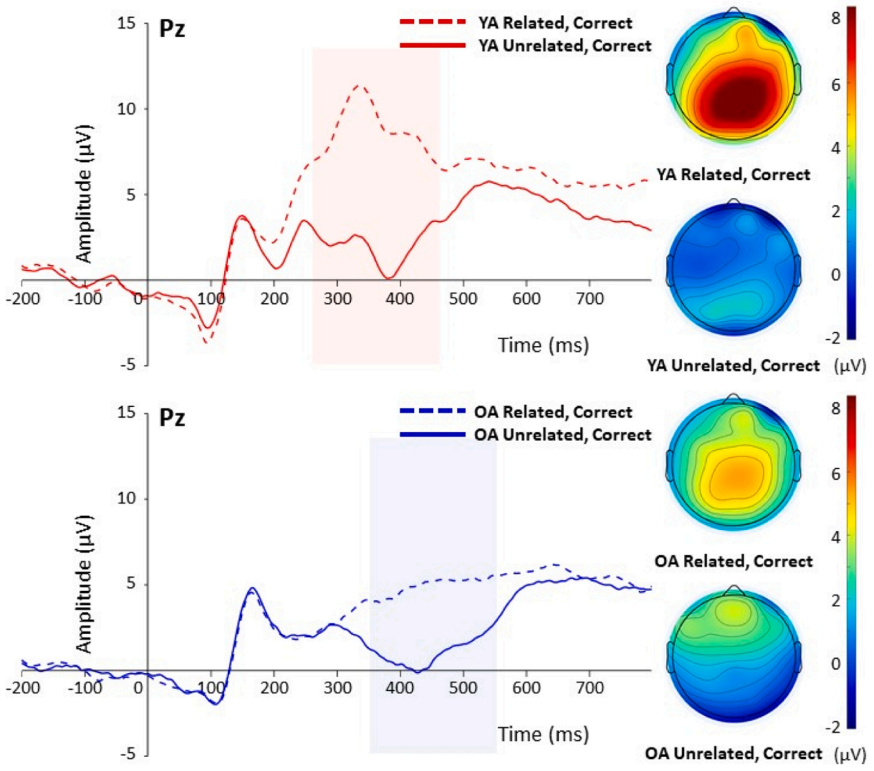

Fig. 6. Word-pair judgment/N400: Grand average waveform plots for Related and Unrelated word-pair conditions produced by younger (YA) and older (OA) adults at Pz. Shaded areas indicate the N400 component time window. Scalp maps represent average voltage for the ERP time window.

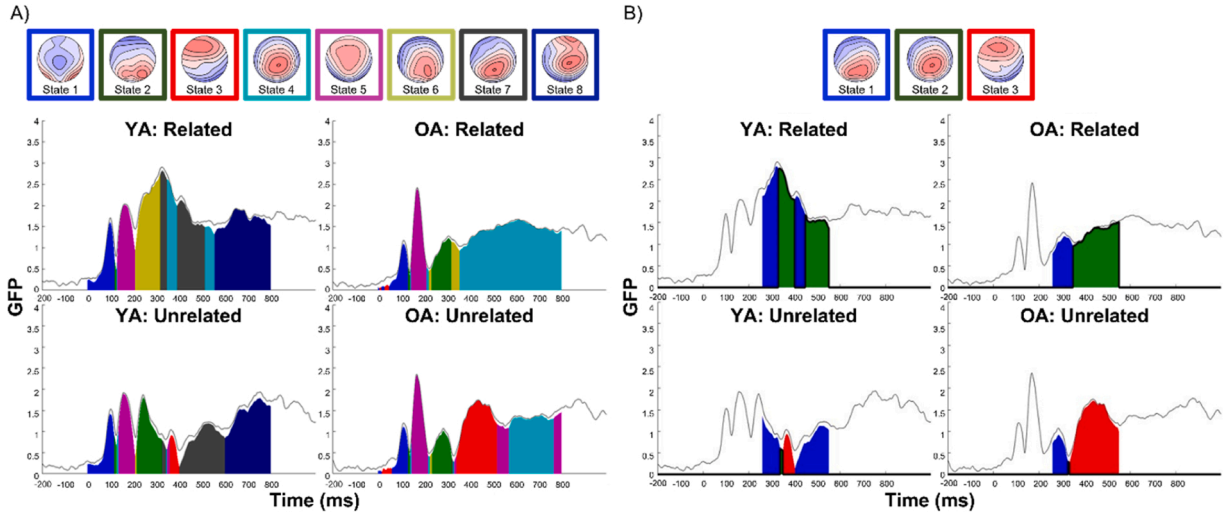

Fig. 7. Word-pair judgment microstate output for younger (YA; left) and older (OA; right) adult groups by Related (upper) and Unrelated (lower) conditions. A) eight states explain 90.75% of total variance for the 0 - 800 ms time period. B) three states explain 91.18% of total variance between 260 - 550 ms.

(Fig. 7A). Constraining the analysis to the 260–550 ms time period, a three-microstate model explained 91.18% of the GFP variance (Fig. 7B). Age groups and conditions shared the same states in a similar order, but differed primarily in State 2 which resembled the centroparietal N400 scalp topography (Kutas and Federmeier, 2011); State 2 was similar to State 4 in the full epoch analysis. State 2 did not produce any Age by Condition interactions; it only showed Condition effects indicating that the Related condition had a longer duration ($p < 0.0001$), greater AUC ($p < 0.0001$), COG ($p < 0.0001$) and mean GFP ($p < 0.0001$) compared to the Unrelated conditions. All of these measures indicated that this centroparietal N400-like topography was had a larger and longer GFP for the Related condition. In contrast, State 3, similar to State 3 in the full epoch, showed a more frontocentral topography, and was only was present for the Unrelated condition. State 3 produced a significant Age by Condition interaction for AUC ($p = 0.02$), indicating that for the Unrelated condition, OAs produced this state more than the YAs. Thus, age appeared to influence measures relating to the occurrence of State 3 with its frontoparietal scalp topography, rather than the state's timing between groups and factor levels.

3.4. Error Processing (ERN)

3.4.1. Behavior

YAs made more errors than OAs, $M_{YA} = 46.06$ (4.69), $M_{OA} = 27.29$ (6.16), $t(32) = 2.43$, $p = 0.02$.

3.4.2. ERN amplitude analyses

We measured pre- and post-response mean amplitudes for correct and error responses at Fz (Gehring et al., 2012; Gentsch et al., 2009). The Age by Condition (Correct, Error) ANOVA (Fig. 8) showed the expected condition effect but no age effect. Both effects were qualified by the significant Age by Condition interaction indicating that the difference between Correct and Error responses was greater for YAs ($p < 0.03$), $M_{\text{YA-Correct}} = -1.52$ μV (0.94), $M_{\text{YA-Error}} = 2.07$ μV (0.76), $M_{\text{OA-Correct}} = 1.18$ μV (0.55), $M_{\text{OA-Error}} = 1.75$ μV (0.83)..

3.4.3. Topographic microstate analyses

The TANOVA indicated no significant Age x Condition interaction during the ERN time period ($p > 0.27$). This lack of interaction suggested that there may be no overlap in stable microstates between age groups during the error processing time period.

Microstate analysis produced six states accounting for 94.71% % of the total variance in GFP for the post-response epoch and three states for the 0–110 ms ERN time period accounting for 94.67% of the total GFP variance. Between 0 to 110 ms, YA and OA groups had little overlap in states, indicating distinct scalp topographies and neural generators for the two age groups. We focus on comparisons of States 1 and 2 that have distributions associated with the ERN. For YAs, the primary state for the ERN was State 2, indicating a frontocentral negativity which had timing and scalp topography consistent with the ERN ERP scalp map of average voltages (Dehaene et al., 1994). State 2 had a significantly longer duration ($p < 0.01$) and AUC ($p < 0.001$) for YAs compared to OAs and there was a significant Age by Condition interaction for duration ($p < 0.003$) and AUC ($p < 0.0001$) indicating that State 2 was present for the YA Error condition compared to the YA correct condition; it was not present for OAs in either condition. State 1 had a frontocentral positive distribution that extended more posteriorally than State 2. State 1 was predominant in the OA's correct and error conditions. The significant Age Group effect for AUC ($p < 0.0001$) indicated that State 2 was produced by OAs rather than YAs. Thus, the significant age-related differences in state behavior were related to the occurrence of specific states rather than their timing.

4. Discussion

Aging has been shown to influence both performance and neural function, but the literature reports mixed results about whether aging has a common effect across cognitive functions or whether it is process specific. In this study we addressed this question by using electroencephalography and a within-subject design to examine age-related changes in neural processing across four different cognitive tasks. Specifically, we used both event-related potential and topographic microstate analytical approaches to examine age-related differences in the timing of neural events and in the topography of neural processing. Although ERP analyses can identify activation in select electrodes, they cannot assess age-related differences in activation across the whole scalp. As a result, we used task-related microstate analyses to classify stable states of whole-head neural activity across time (Murray et al., 2008; Michel and Koenig, 2018). Microstate analyses provided additional insights into age-related changes in the distribution of whole-head

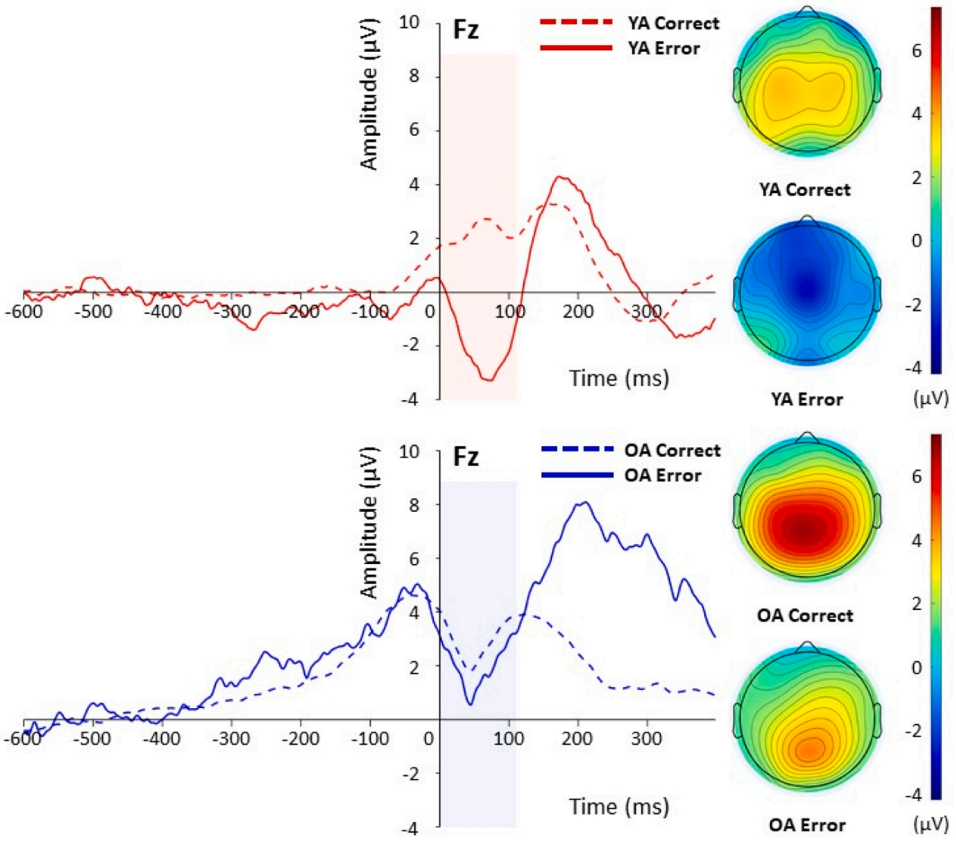

Fig. 8. Flanker/ERN: Grand average waveform plots for Correct and Error response conditions produced by younger (YA) and older (OA) adults at Fz (baseline is −600 to −400). Peak-to-peak mean amplitudes are calculated as the difference between the mean amplitude − 110 to 0 ms prior to response and the mean amplitude 0 to 110 ms following the response. Scalp maps represent average voltage for the shaded ERP time window.

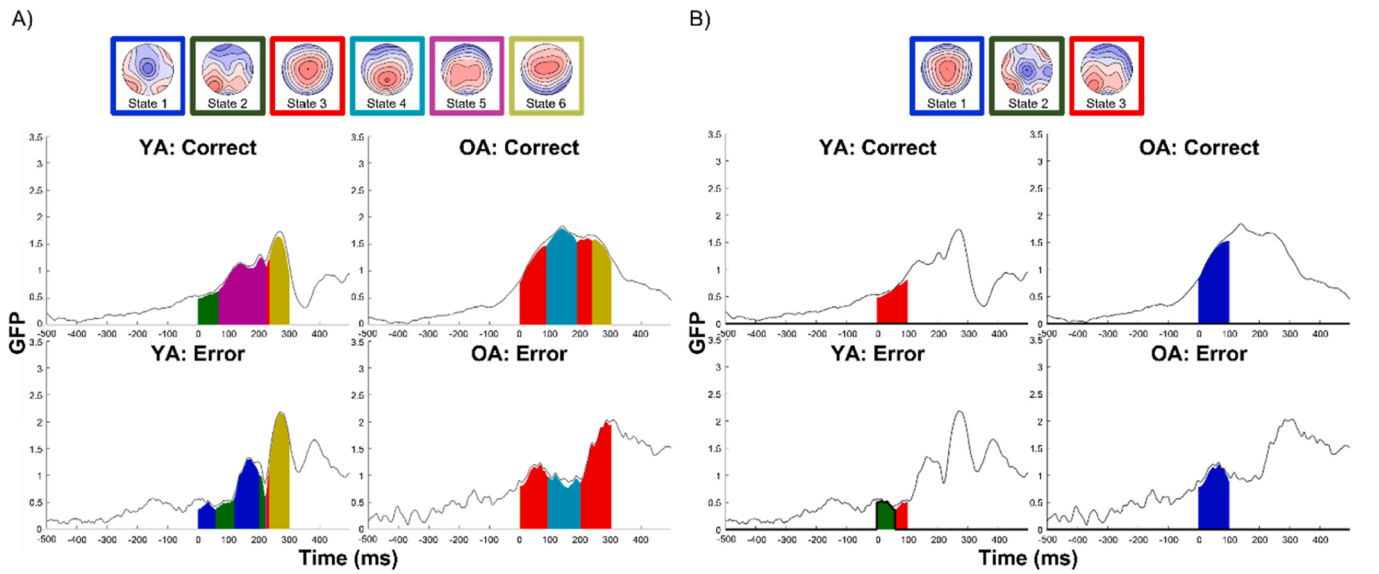

Fig. 9. Response-locked flanker task/ERN microstate output for younger (YA; left) and older (OA; right) adult groups by Correct (upper) and Error (lower) responses. A) Six states explain 94.71% of total variance for the 0 - 300 ms time period. B) Three states explain 94.67% of total variance between 0 - 110 ms.

neural activity beyond those provided by ERP analyses. Results from both ERP and topographical microstate indicated that age effects on neural responses were not uniform across the tasks.

For face perception, age-related differences were associated with small processing delays rather than with the strength or the topography of the neural processing. We found no age-related differences in the effects of condition (face vs. car) or hemisphere. In the literature, evidence for age-related differences in N170 amplitudes and hemispheric specialization is mixed (Boutet et al., 2021; Daniel and Bentin, 2012). Microstate analysis confirmed the same microstates for both age groups, emerging in the same order. The predominant occipitotemporal microstate was similar to the N170 scalp distribution for a similar time period (Rossion and Jacques, 2008). Although the onset of the microstate was similar, the microstate had a longer duration for older adults. Thus, ERP and topographic analysis converge on the finding that for the more perceptual encoding of objects, aging influences the timing (Pichot et al., 2022), but not the neural generators associated with face processing.

For attention and categorization, as measured by the visual oddball task, ERP analyses confirmed overall age-related delays in the P3 (van Dinteren et al., 2014), as well as an age by condition interaction arising from a larger difference between rare and frequent events in younger adults. Microstate analyses demonstrated age-related timing and strength differences in the scalp topographies over time. Both voltage maps and microstate maps showed a different pattern of centroparietal activation for OAs than YAs, a pattern that extended across more electrodes both frontally and laterally. However, unlike other aging studies using fMRI methodology (Reuter-Lorenz and Lustig, 2017), the activation did not move or extend to frontal pole areas.[2] Microstate analyses also showed less differentiation in GFP between conditions for OAs compared to YAs. OAs may not orient as strongly to infrequent stimuli, such that they do not evaluate as big a discrepancy between rare stimuli and the context, defined by the frequent stimuli.

Semantic processing was measured by a word-pair judgment task in which the N400 is a cognitive index of automatic semantic activation. ERP analyses also replicated delayed, smaller N400 effects for OAs than Yas (Tiedt et al., 2020). The age-related difference occurred because amplitudes were similar for YAs and OAs with unrelated pairs but were much larger in YAs than OAs for related pairs. Joyal et al. (2020) also reported an influence of age on the N400 difference wave, but it is unclear if the age-related difference was driven by the related condition in their study as it was in ours. Microstate analyses further confirmed that both age groups produced a common microstate (State 2) with a tight centroparietal distribution of activity. This state was present with related word pairs but not with unrelated pairs. However, a different microstate (State 3) with a more frontocentral distribution distinguished the OAs from the YAs in the unrelated condition. These age-related differences suggest an anterior spread in older adults' activation but only for evaluating unrelated word pairs. Thus, for attention/categorization (P3) and semantic processing (N400), microstate analyses indicated age differences in processing states. During critical time windows of processing, older adult states showed more widely spread centroparietal scalp distributions that moved anteriorly relative to those of younger adults.

Unlike the above stimulus-locked tasks, ERPs elicited from the flanker task were response-locked. The flanker task isolated neural activity associated with error responses. The ERN ERP analyses indicated age-related differences in processing correct and error responses: Older adults show a smaller difference than young adults. Importantly, microstate analysis revealed distinctly different microstates between older and younger adults, something only implied by the ERP analyses. OAs showed the same central positivity for error and correct responses whereas YAs showed central negativity for error responses but a left-lateralized state for correct responses. Hoffmann and Falkenstein (2011) found the ERN ERP had a somewhat different component structure for older adults and this difference is apparent in the microstate analyses, which classified the topography of activity across the scalp as significantly differing across groups. For younger adults, the ERN produced a microstate with frontocentral negativity, but for older adults, the relevant microstate showed a frontocentral relative positivity.

In sum, this study extended the limited research examining task-related microstates (rather than resting-state, Zanesco et al., 2020; Jabès et al., 2021) to explore age-related differences in neural processing. By comparing the results from ERP and microstate analyses across tasks, we have shown that microstate analysis provides greater context to the ERP analyses because it does not require having to make a priori assumptions about electrodes of interest and time windows. We used

[2] Of interest, although we did not report this comparison, there was no statistical difference across Cz, CPz, and Pz electrodes within each age group for P3 amplitudes, despite the apparent microstate and voltage differences.

well-established ERPs elicited from stable paradigms and microstates were shown to provide converging evidence for the scalp distribution and timing of the neural effects. However, they also contributed to our understanding of those effects that change with age.

Several frameworks have been proposed to account for age-related differences in brain activation (Festini et al., 2018; Oosterhuis et al., 2023): central nervous system slowing (CNSS); dedifferentiation (DD, Koen et al., 2020), posterior-to-anterior shift in aging (PASA; Davis et al., 2008), hemispheric asymmetry reduction in older adults (HAROLD; Cabeza, 2002), diffused activation (DA; Voss et al., 2008), compensation-related utilization of neural circuits (CRUNCH; Reuter--Lorenz and Cappell, 2008), and the scaffolding theory of aging and cognition (STAC, Park and Reuter-Lorenz (2009), and STAC-r[evised] (Reuter-Lorenz and Park, 2014).

CNSS proposes a general slowing of neuronal transmission in the central nervous system (Birren and Fisher, 1995; Salthouse, 1996). It predicts that the latency of neural events will be longer in older adults. Dedifferentiation is signaled when the effect of a manipulation is stronger in younger than in older adults (Koen and Rugg, 2019). The distinctiveness of neural responses is reduced in older adults, such that brain activation patterns are less specific to a particular type of input or mental state. Closely related concepts refer to a loss of neural coherence and increased neural noise with increasing age (Layton, 1975). Diffused activation is closely related to dedifferentiation and often the terms are used interchangeably (Voss et al., 2008). Here we use DA to refer to topographical patterns that have similar foci (as opposed to different foci) in the two age groups, but a greater spread in the older adults. Although DD may result in DA, the presence of DA does not necessarily entail DD (Koen and Rugg, 2019). PASA describes patterns in which tasks elicit posterior, parietal activation in younger adults but frontal activity in older adults. HAROLD notes greater bilateral activation (especially frontal) in older adults where activation is more unilateral in younger adults. For example, Reuter-Lorenz et al. (2000) found that spatial working memory was right-lateralized in frontal cortex in younger adults whereas verbal working memory was left-lateralized but both tasks elicited bilateral activation in older adults. CRUNCH postulates that the level of brain activation in response to increased task demands increases regardless of age. Older adults, with already reduced resources, should show this recruitment at lower levels of demand. The STAC views cognitive activity as being embedded in a scaffold consisting of individual differences in brain integrity, compensatory activation, maintenance, education, and richness of experience. DA, PASA, and HAROLD make predictions about the topographical foci of cortical activity and microstate analysis is uniquely suited to assess their fit to the data. CRUNCH is consistent with all three, and further, explains why the patterns of activation are different in younger and older adults. STAC-r could encompass all of the above, depending on the task, the person, neural changes, recruitment, and other factors. Patterns consistent with PASA, HAROLD, and CRUNCH are often elicited by tasks with a high cognitive demand, whereas all of our tasks were less cognitively demanding. Nevertheless, Reed et al. (2017) found a pattern apparently consistent with PASA using a simple detection task.

Our datasets comprising four different cognitive domains and processes provide a unique opportunity to compare and contrast these frameworks. Microstates help to differentiate among these theories. The slowing of neural transmission postulated by CNSS would be signaled by longer latencies for ERPs and delayed onsets of microstates in older adults. This was found in the face perception (N170), attention (P3), and categorization (N400) experiments. In the flanker response processing (ERN/CRN) experiment, RTs were clearly longer for OAs, but the response-related processing was carried out in the same window for both OAs and YAs.

DD would be signaled primarily by smaller effects of the condition manipulations in OAs than in YAs. This was found in the P3, N400, and ERN/CRN experiments. For P3, rare minus frequent was larger for YAs (7.41 μV) than for OAs (4.52 μV); for N400, related minus unrelated was larger for YAs (6.87 μV) than for OAs (3.90 μv); for ERN/CRN, correct minus error was larger for YAs (3.59 μV) than for OAs (0.57 μV). By contrast, for N170 faces minus cars was greater in magnitude for OAs (−2.50 μV) than for YAs (−1.21 μV) although the interaction of age group and condition did not reach significance. A plausible interpretation is that more perceptual tasks show less evidence of dedifferentation.

Topographical patterns would be classified as DA when YAs and OAs have similar foci but the spread of activation is greater in the OAs. Only the P3 experiment fit this pattern. Activation in OAs (State 3) was more diffuse than in YAs (State 2), extending slightly frontally but also more posteriorally and laterally. The same states were active with both frequent and rare stimuli. It should be noted that the activation was more parietal in OAs and more central in YAs. Activation in the ERN/CRN experiment was more diffuse for OAs but it had a clearly different focus than the YAs.

Only the N400 experiment clearly fit the pattern described by PASA. For related word pairs YAs and OAs show the same state with a parietal focus. For OAs but not YAs, the presumably more difficult unrelated word pairs elicited a clear frontal focus. In the P3 experiment, as noted, activation for OAs was shifted slightly forward— a pattern that might be interpreted as consistent with PASA— although the focus was central rather than frontal.

Evidence consistent with HAROLD was also found in only one experiment, ERN/CRN. Here YAs showed focused activation in left occipital-parietal cortex. A true HAROLD pattern would have focused activation in OAs in both left and right occipital-parietal cortex. Instead, the activation for OAs was central and diffuse for both correct and error responses.

The patterns of age-related differences that were most consistent across experiments, then, were those characterized by the slowing and dedifferentiation frameworks. The microstate analyses showed that the three experiments other than face perception (N170) were each characterized by a different pattern of age-related differences in topography: the oddball attention task (P3) showed a diffuse activation pattern; the semantic categorization task (N400) showed a PASA pattern; the flanker task (ERN/CRN) arguably showed a HAROLD pattern. It is important to remember that the same participants completed all four tasks at the same time. This underscores the conclusion that different cognitive tasks elicit different topographies of age-related differences. The findings as a whole—evidence across tasks for slowing and dedifferentation as well as different topographies for different tasks—are well accounted for by the STAC-r framework, acknowledging as it does the interacting contributions of fundamental nervous system changes, of strategic responses to task demands, and of life experiences.

4.1. Conclusion

In conclusion, we examined whether different cognitive tasks would reveal similar or different age-related differences in neural responses. Our classic ERP-evoking tasks provided known timing and loci of neural processing, thereby allowing us to confirm the outputs of the microstate analyses. The state maps from topographical microstate analysis provided additional insight into the spatial distribution of electrical activity across the whole scalp during different phases of neural processing, especially regarding the onset, offset, and power of the stable microstates. This technique clarified the dynamics of neural activity and provided insights into the organization of cognitive and neural processes.

When compared to traditional ERPs, microstates can provide additional information from the ERPs in three major ways. First, microstates take into account activation across the whole scalp relative to the activation from a single or small group of electrodes. The microstate approach does not have a priori assumptions as to the distribution of scalp activations. Second, if the two groups and conditions share common microstates, then the scalp distributions can speak quantitatively to the strength, onset and duration of specific microstates. We observed

such timing and strength differences for face and object processing and the N170. Third, if the two groups and conditions have different microstates, then the scalp distributions in the microstates can speak to the changes in underlying neural activation/generators producing different patterns of activation. We observed these activation pattern differences in for context updating/P3, semantic judgments/N400, and error processing/ERN.

In contrast to ERPs or microstates, fMRI allows the identification of specific loci that are engaged by a task. The theoretical frameworks, though, make broader claims about general areas of activation such as frontal or lateral. With some cautions, EEG/ERP topographies can speak to such claims. Our goal here was to understand the age-related differences we found using ERPs and microstates using the aging theories as a contextual framework. The areas of cortical activation found in this study are consistent with those found in fMRI studies. With microstate analysis, we were able to characterize the moment to moment changes in the patterns of activation over short periods of time.

Microstate analyses, as well as the ERP analyses, showed different effects of age across tasks which were most consistent with the STAC-r framework that proposes age-related effects differ depending on the resources available and the kinds of processing and cognitive load required of various tasks. As noted, however, our tasks placed less demand on executive function than many of the tasks (e.g., working memory tasks) from which some of these frameworks were developed, which may explain why we did not observe frontal recruitment. The ERP data suggest differences in the brain's response to age-related neural changes under different cognitive demands. For each cognitive task, microstate analysis quantified when age influenced the timing and scalp distribution of the neural response. The important contribution of this study is as a proof of concept that task-related microstate analysis can show age similarities and differences in processing states not captured by ERP analysis. Additional studies using ERP and microstate analyses with a larger participant sample and with systematic manipulation of task difficulty could inform current theories of aging in terms of the conditions under which different types of neural compensation are elicited.

Funding

This work was supported by the National Science Foundation (NSF DUE 1626554, 1822381, 1914855, and 2227412). Thanks to Cindy Bukach, Jane Couperus, and the members of the PURSUE project (pursueerp.com), CMC Summer Research Program, and Carleton Summer Research Program for their support of this project.

CRediT authorship contribution statement

Hartley Alan A.: Writing – review & editing, Writing – original draft, Visualization, Validation, Methodology, Investigation, Formal analysis, Conceptualization. **Petropoulos Astrid:** Writing – review & editing, Formal analysis. **Thapar Anjali:** Writing – review & editing, Conceptualization. **Denaro Chandlyr M.:** Writing – review & editing, Writing – original draft, Visualization, Validation, Project administration, Methodology, Investigation, Formal analysis, Data curation, Conceptualization. **Joshi Jasmin:** Writing – review & editing, Formal analysis. **Reed Catherine L:** Writing – review & editing, Writing – original draft, Visualization, Validation, Supervision, Software, Resources, Project administration, Methodology, Investigation, Funding acquisition, Formal analysis, Data curation, Conceptualization.

Declaration of Competing Interest

None of the authors have conflicts of interest.

Acknowledgments

None.

References

Banaschewski, T., Brandeis, D., 2007. Annotation: what electrical brain activity tells us about brain function that other techniques cannot tell us: A child psychiatric perspective. J. Child Psychol. Psychiatry 48, 415-35. https://doi.org/10.1111/j.1469-7610.2006.01681.x.

Birren, J.E., Fisher, L.M., 1995. Aging and speed of behavior: possible consequences for psychological functioning. Annu Rev. Psychol. 46, 329–53. https://doi.org/10.1146/annurev.ps.46.020195.001553.

Boutet, I., Shah, D.K., Collin, C.A., Berti, S., Persike, M., Meinhardt-Injac, B., 2021. Age-related changes in amplitude, latency and specialization of ERP responses to faces and watches. Aging, Neuropsychol. Cogn. 28 (1), 27–64. https://doi.org/10.1080/13825585.2019.1708253.

Brandeis, D., Lehmann, D., Michel, C.M., Mingrone, W., 1995. Mapping event-related brain potential microstates to sentence endings. Brain Topogr. 8 (2), 145–159. https://doi.org/10.1007/BF01199778.

Cabeza, R., 2002. Hemispheric asymmetry reduction in older adults: the HAROLD model. Psychol. Aging 17 (1), 85–100. https://doi.org/10.1037//0882-7974.17.1.85.

Chaumon, M., Bishop, D.V., Busch, N.A., 2015. A practical guide to the selection of independent components of the electroencephalogram for artifact correction. J. Neurosci. Methods 250, 47–63. https://doi.org/10.1016/j.jneumeth.2015.02.025.

, 1976CIE, 1976. Official Recommendations on Uniform Colour Spaces, Colour Differences Equations, and Metric Colour Terms. In: Supplement, 2. to CIE Publication, No.15, Paris.

Custo, A., Van De Ville, D., Wells, W.M., Tomescu, M.I., Brunet, D., Michel, C.M., 2017. Electroencephalographic resting-state networks: source localization of microstates. Brain Connect 7, 671–682. https://doi.org/10.1089/brain.2016.0476.

Daniel, S., Bentin, S., 2012. Age-related changes in processing faces from detection to identification: ERP evidence. Neurobiol. Aging 33 (1), 206.e1–206.e28. https://doi.org/10.1016/j.neurobiolaging.2010.09.001.

Davis, S.W., Dennis, N.A., Daselaar, S.M., Fleck, M.S., Cabeza, R., 2008. Que PASA? The posterior-anterior shift in aging. Cereb. Cortex 18 (5), 1201–1209. https://doi.org/10.1093/cercor/bhm155.

Dehaene, S., Posner, M.I., Tucker, D.M., 1994. Localization of a neural system for error detection and compensation. Psych. Sci. 5 (5), 303–305. https://doi.org/10.1111/j.1467-9280.1994.tb00630.x.

Delorme, A., Makeig, S., 2004. EEGLAB: an open-source toolbox for analysis of single-trial EEG dynamics including independent component analysis. J. Neurosci. Methods 134 (1), 9–21. https://doi.org/10.1016/j.jneumeth.2003.10.009.

Delorme, A., Sejnowski, T., Makeig, S., 2007. Enhanced detection of artifacts in EEG data using higher-order statistics and independent component analysis. NeuroImage 34 (4), 1443–1449. https://doi.org/10.1016/j.neuroimage.2006.11.004.

Eimer, M., 2011. The face-sensitivity of the n170 component. Front. Hum. Neurosci. 18 (5), 119. https://doi.org/10.3389/fnhum.2011.00119.

Eriksen, B.A., Eriksen, C.W., 1974. Effects of noise letters upon the identification of a target letter in a nonsearch task. Percept. Psychophys. 16 (1), 143–149. https://doi.org/10.3758/BF03203267.

Festini, S.B., Zahodene, L., Reuter-Lorenz, P.A., 2018. Theoretical perspectives on age differences in brain activation: HAROLD, PASA, CRUNCH – how do they STAC up? Oxf. Res. Encycl. Psychol. https://doi.org/10.1093/acrefore/9780190236557.013.400.

Feuerriegel, D., Churches, O., Hofmann, J., Keage, H.A.D., 2015. The N170 and face perception in psychiatric and neurological disorders: a systematic review. Clin. Neurophysiol. 126 (6), 1141–1158. https://doi.org/10.1016/j.clinph.2014.09.015.

Friedman, D., 2012. The components of aging. In: Luck, S., Kappenman E, S. (Eds.), The Oxford Handbook of Event-related Potential Components. Oxford Press, New York, pp. 514–536.

Gehring, W.J., Liu, Y., Orr, J.M., Carp, J., 2012. The error related negativity (ERN/Ne). In: Luck, S.J., Kappenman, E.S. (Eds.), The Oxford Handbook of Event-Related Potential Components. Oxford University Press, pp. 231–291. https://doi.org/10.1177/17456916177153.

Gentsch, A., Ullsperger, P., Ullsperger, M., 2009. Dissociable medial frontal negativities from a common monitoring system for self- and externally caused failure of goal achievement. NeuroImage 47 (4), 2023–2030. https://doi.org/10.1016/j.neuroimage.2009.05.064.

Grady, C., 2012. The cognitive neuroscience of ageing. Nat. Rev. Neurosci. 13, 491–505. https://doi.org/10.1038/nrn3256.

Harnish, M.J., Beatty, W.W., Nixon, S.J., Parsons, O.A., 1994. Performance by normal subjects on the Shipley institute of living scale. J. Clin. Psych. 50 (6), 881–883. https://doi.org/10.1002/1097-4679(199411)50:6<881::AID-JCLP2270500611>3.0.CO;2-4.

Hoffmann, S., Falkenstein, M., 2011. Aging and error processing: age related increase in the variability of the error-negativity is not accompanied by increase in response variability. PLOS One 6 (2), e17482. https://doi.org/10.1371/journal.pone.0017482.

Hong, X., Sun, J., Bengson, J.J., Tong, S., 2014. Age-related spatiotemporal reorganization during response inhibition. Int. J. Psychophysiol. 93, 371–380. https://doi.org/10.1016/j.ijpsycho.2014.05.013.

Jabès, A., Klencklen, G., Ruggeri, P., Michel, C.M., Lavenex, P.B., Lavenex, P., Resting-state, E.E.G., 2021. microstates parallel age-related differences in allocentric spatial

working memory performance. Brain Topogr. 34, 442–460. https://doi.org/10.1007/s10548-021-00835-3.
Jacques, C., Rossion, B., 2004. Concurrent processing reveals competition between visual representations of faces. NeuroReport 15 (15), 2417–2421. https://doi.org/10.1097/00001756-200410250-00023.
Jouen, A.L., Lancheros, M., Laganaro, M., 2021. Microstate ERP analyses to pinpoint the articulatory onset in speech production. Brain Topogr. 34, 29–40. https://doi.org/10.1007/s10548-020-00803-3.
Joyal, M., Groleau, C., Bouchard, C., Wilson, M.A., Fecteau, S., 2020. Semantic processing in healthy aging and Alzheimer's disease: a systematic review of the N400 differences. Brain Sci. 10 (11), 770. https://doi.org/10.3390/brainsci10110770.
Jung, T.P., Makeig, S., Humphries, C., Lee, T.W., McKeown, M.J., Iragui, V., Sejnowski, T.J., 2000. Removing electroencephalographic artifacts by blind source separation. Psychophysiology 37 (2), 163–178. https://doi.org/10.1111/1469-8986.3720163.
Kappenman, E.S., Farrens, J.L., Zhang, W., Stewart, A.X., Luck, S.J., 2021. ERP CORE: an open resource for human event-related potential research. NeuroImage 225, 117465. https://doi.org/10.1016/j.neuroimage.2020.117465.
Khanna, A., Pascual-Leone, A., Michel, C.M., Farzan, F., 2015. Microstates in resting-state EEG: current status and future directions. Neurosci. Biobehav Rev. 49, 105–113. https://doi.org/10.1016/j.neubiorev.2014.12.010.
Kim, K., Duc, N.T., Choi, M., et al., 2021. EEG microstate features according to performance on a mental arithmetic task. Sci. Rep. 11, 343. https://doi.org/10.1038/s41598-020-79423-7.
Koen, J.D., Rugg, M.D., 2019. Neural dedifferentiation in the aging brain. Trends Cogn. Sci. 23 (7), 547–559. https://doi.org/10.1016/j.tics.2019.04.012.
Koen, J.D., Srokova, S., Rugg, M.D., 2020. Age-related neural dedifferentiation and cognition. Curr. Opin. Behav. Sci. 32, 7–14. https://doi.org/10.1016/j.cobeha.2020.01.006.
Koenig, T., Kottlow, M., Stein, M., Melie-García, L., 2011. Ragu: a free tool for the analysis of EEG and MEG event-related scalp field data using global randomization statistics. Comput. Intell. Neurosci., 938925 https://doi.org/10.1155/2011/938925.
Koenig, T., Studer, D., Hubl, D., Melie, L., Strik, W.K., 2005. Brain connectivity at different time-scales measured with EEG. Philos. Trans. R. Soc. Lond. B Bio Sci. 360, 1015–1024. https://doi.org/10.1098/rstb.2005.1649.
Koenig, T., Prichep, L., Lehmann, D., Sosa, P.V., Braeker, E., Kleinlogel, H., Isenhart, R., John, E.R., 2002. Millisecond by millisecond, year by year: normative EEG microstates and developmental stages. Neuroimage 16 (1), 41–48. https://doi.org/10.1006/nimg.2002.1070.
Kropotov, J., Ponomarev, V., Tereshchenko, E.P., Müller, A., Jäncke, L., 2016. Effect of aging on ERP components of cognitive control. Front. Aging Neurosci. 8. https://doi.org/10.3389/fnagi.2016.00069.
Kutas, M., Hillyard, S.A., 1980. Reading senseless sentences: brain potentials reflect semantic incongruity. Science 207 (4427), 203–5. https://doi.org/10.1016/0301-0511(80)90046-0.
Kutas, M., Federmeier, K.D., 2011. Thirty years and counting: finding meaning in the N400 component of the event-related brain potential (ERP). Annu Rev. Psychol. 62, 621-47. https://doi.org/10.1146/annurev.psych.093008.131123.
Lau, E.F., Phillips, C., Poeppel, D., 2008. A cortical network for semantics: (de) constructing the N400. Nat. Rev. Neurosci. 9 (12), 920-33. https://doi.org/10.1038/nrn2532.
Layton, B., 1975. Perceptual noise and aging. Psychol. Bull. 82 (6), 875–883. https://doi.org/10.1037/0033-2909.82.6.875.
Lehmann, D., Michel, C.M., 2011. EEG-defined functional microstates as basic building blocks of mental processes. Clin. Neurophysiol. 122 (6), 1073–1074. https://doi.org/10.1016/j.clinph.2010.11.003.
Ménétré, E., Laganaro, M., 2023. The temporal dynamics of the Stroop effect from childhood to young and older adulthood. PLOS One 18 (3), e0256003. https://doi.org/10.1371/journal.pone.0256003.
Michel, C.M., Koenig, T., 2018. EEG microstates as a tool for studying the temporal dynamics of whole-brain neuronal networks: a review. NeuroImage 180 (Pt B), 577–593. https://doi.org/10.1016/j.neuroimage.2017.11.062.
Murray, M.M., Brunet, D., Michel, C.M., 2008. Topographic ERP analyses: a step-by-step tutorial review. Brain Topogr. 20, 249–264. https://doi.org/10.1007/s10548-008-0054-5.
Olvet, D.M., Hajcak, G., 2008. The error-related negativity (ERN) and psychopathology: toward an endophenotype. Clin. Psychol. Rev. 28 (8), 1343–1354. https://doi.org/10.1016/j.cpr.2008.07.003.
Oosterhuis, E., Slade, K., Smith, E., May, P.J.C., Nuttall, H.E., 2023. Toward an understanding of healthy cognitive aging: the importance of lifestyle in cognitive reserve and the scaffolding theory of aging and cognition. J. Gerontol. B 78 (5), 777–778. https://doi.org/10.1093/geronb/gbac197.
Paitel, E.R., Samii, M.R., Nielson, K.A., 2021. A systematic review of cognitive event-related potentials in mild cognitive impairment and Alzheimer's disease. Behav. Brain Res. 396, 112904 https://doi.org/10.1016/j.bbr.2020.11290.
Park, D.C., Reuter-Lorenz, P., 2009. The adaptive brain: aging and neurocognitive scaffolding. Ann. Rev. Psychol. 60, 173–196. https://doi.org/10.1146/annurev.psych.59.103006.093656.
Pichot, R.E., Henreckson, D.J., Foley, M., Koen, J.D., 2022. Neural noise is associated with age-related neural dedifferentiation. bioRxiv. https://doi.org/10.1101/2022.11.17.516990.
Pion-Tonachini, L., Kreutz-Delgado, K., Makeig, S., 2019. ICLabel: An automated electroencephalographic independent component classifier, dataset, and website. Neuroimage 198, 181–197. https://doi.org/10.1016/j.neuroimage.2019.05.026.
Polich, J., 2007. Updating P300: an integrative theory of P3a and P3b. Clin. Neurophysiol. 118 (10), 2128–2148. https://doi.org/10.1016/j.clinph.2007.04.019.
Polich, J., 2012. Neuropsychology of P300. In: Kappenan, E.S., Luck, S.J. (Eds.), The Oxford Handbook of Event-Related Potential Components. https://doi.org/10.1093/oxfordhb/9780195374148.013.0089.
Reed, C.L., Clay, S.N., Leland, D.S., Kramer, A., Hartley, A.A., 2017. Attentional effects of hand proximity occur later in older adults: evidence from event-related potentials. Psych. Aging 32 (8), 710–721. https://doi.org/10.1037/pag0000207.
Reuter-Lorenz, P., Cappell, K., 2008. Neurocognitive aging and the compensation hypothesis. Cur Dir. Psychol. Sci. 17 (3), 177–182. ⟨https://www.jstor.org/stable/20183277⟩.
Reuter-Lorenz, P.A., Park, D.C., 2014. How does it STAC up? Revisiting the scaffolding theory of aging and cognition. Neuropsychol. Rev. 24 (3), 355–370. https://doi.org/10.1007/s11065-014-9270-9.
Reuter-Lorenz, P.A., Lustig, C., 2017. Working memory and executive functions in the aging brain. In: Cabeza, R., Nyberg, L., Park, D.C. (Eds.), Cognitive Neuroscience of Aging: Linking Cognitive and Cerebral Aging., second ed. Oxford University Press, MA, pp. 235–258 (https://doi-org.ccl.idm.oclc.org/10.1093/acprof:oso/9780199372935.003.0010).
Reuter-Lorenz, P.A., Jonides, J., Smith, E.E., Hartley, A., Miller, A., Marshuetz, C., Koeppe, R.A., 2000. Age differences in the frontal lateralization of verbal and spatial working memory revealed by PET. J. Cogn. Neurosci. 12 (1), 174–187. https://doi.org/10.1162/089892900561814.
Reuter-Lorenz, PA, Park, DC, 2010. Human neuroscience and the aging mind: a new look at old problems. J Gerontol B Psychol Sci Soc Sci 65 (4), 405–415. https://doi.org/10.1093/geronb/gbq035.
Rossion, B., Jacques, C., 2008. Does physical interstimulus variance account for early electrophysiological face sensitive responses in the human brain? Ten lessons on the N170. NeuroImage 39, 1959–1979.
Rossion, B., Caharel, S., 2011. ERP evidence for the speed of face categorization in the human brain: disentangling the contribution of low-level visual cues from face perception. Vis. Res. 51 (12), 1297–1311. https://doi.org/10.1016/j.visres.2011.04.003.
Rossion, B., Jacques, C., 2012. The N170: Understanding the time course of face perception in the human brain. In: Luck, S.J., Kappenman, E.S. (Eds.), The Oxford Handbook of Event-Related Potential Components. Oxford University Press, pp. 115–141. https://doi.org/10.1093/oxfordhb/9780195374148.013.0064.
Rossion, B., Joyce, C.A., Cottrell, G.W., Tarr, M.J., 2003. Early lateralization and orientation tuning for face, word, and object processing in the visual cortex. Neuroimage 20, 1609–1624. https://doi.org/10.1016/j.neuroimage.2003.07.010.
Salthouse, T.A., 1996. The processing-speed theory of adult age differences in cognition. Psych. Rev. 103 (3), 403–428. https://doi.org/10.1037/0033-295x.103.3.403.
Shipley, W.C., Burlingame, C.C., 1941. A convenient self-administered scale for measuring intellectual impairment in psychotics. Am. J. Psychiatry 97, 1313–1325. https://doi.org/10.1176/ajp.97.6.1313.
Skrandies, W., 1990. Global field power and topographic similarity. Brain Topogr. 3, 137–141. https://doi.org/10.1007/BF01128870.
Staub, B., Doignon-Camus, N., Bacon, E., Bonnefond, A., 2014. Investigating sustained attention ability in the elderly by using two different approaches: inhibiting ongoing behavior versus responding on rare occasions. Acta Psychol. 146, 51–57. https://doi.org/10.1016/j.actpsy.2013.12.003.
Swaab, T.Y., Ledoux, K., Camblin, C.C., Boudewyn, M.A., Language-Related, E.R.P., 2011. Components. In: Kappenman, E.S., Luck, S.J. (Eds.), The Oxford Handbook of Event-Related Potential Components. Oxford Library of Psychology. https://doi.org/10.1093/oxfordhb/9780195374148.013.0197.
Tiedt, H.O., Ehlen, F., Klostermann, F., 2020. Age-related dissociation of N400 effect and lexical priming. Sci. Rep. 10 (1), 20291. https://doi.org/10.1038/s41598-020-77116-9.
Tomescu, M.I., Rihs, T.A., Rochas, V., Hardmeier, M., Britz, J., Allali, G., Fuhr, P., Eliez, S., Michel, C.M., 2018. From swing to cane: sex differences of EEG resting-state temporal patterns during maturation and aging. Dev. Cogn. Neurosci. 31, 58–66. https://doi.org/10.1016/j.dcn.2018.04.011.
van Dinteren, R., Arns, M., Jongsma, M.L., Kessels, R.P., 2014. P300 development across the lifespan: a systematic review and meta-analysis. PLOS One 9 (2), e87347. https://doi.org/10.1371/journal.pone.0087347.
Voss, M.W., Erickson, K.I., Chaddock, L., Prakash, R.S., Colcombe, S.J., Morris, K.S., Doerksen, S., Hu, L., McAuley, E., Kramer, A.F., 2008. Dedifferentiation in the visual cortex: an fMRI investigation of individual differences in older adults. Brain Res. 1244, 121–131. https://doi.org/10.1016/j.brainres.2008.09.051.
Wang, Y., Huang, H., Yang, H., Xu, J., Mo, S., Lai, H., Wu, T., Zhang, J., 2019. Influence of EEG references on N170 component in human facial recognition. Front. Neurosci. 13, 705. https://doi.org/10.3389/fnins.2019.00705.
Yi, Y., Friedman, D., 2011. Age-related differences in working memory: ERPs reveal age-related delays in selection- and inhibition-related processes. Aging Neuropsychol. Cogn. 21 (4), 483–513. https://doi.org/10.1080/13825585.2013.833581.
Zanesco, A.P., King, B.G., Skwara, A.C., Saron, C.D., 2020. Within and between-person correlates of the temporal dynamics of resting EEG microstates. Neuroimage 211, 116631. https://doi.org/10.1016/j.neuroimage.2020.116631.